

Design of Acoustic Metamaterials based on the Concept of Dual Transmission Line

Anne-Sophie Moreau¹, Hervé Lissek^{*1}, and Frédéric Bongard²

¹Ecole Polytechnique Fédérale de Lausanne, EPFL-STI-IEL-LEMA, Station 11, CH-1015 Lausanne, Switzerland

²JAST SA, PSE-EPFL, Bat. C, CH-1015 Lausanne, Switzerland

*Corresponding author: herve.lissek@epfl.ch

Abstract: Within the last years, an increasing number of studies have been carried out in the field of acoustic metamaterials. These artificial composite materials aim at achieving new macroscopic properties, like negative refraction, that are not readily present in nature. In analogy to electromagnetics, where such concepts are more mature, a novel concept of artificial acoustic transmission line has recently been reported, which presents such artificial behavior. In this article, the design of the proposed transmission line is presented and a validation is made with the help of a finite element model. Moreover, these results are compared to a usual circuit description of the problem. One cell and 10-cell long structures are implemented in Comsol Multiphysics® and confirm the good performances of the different models, in terms of dispersion diagram, Bloch impedance, as well as reflection and transmission coefficients.

Keywords: acoustic metamaterial, transmission line, finite element model, negative refraction.

1 Introduction

Metamaterials are defined as artificial composite materials designed to achieve new macroscopic properties that are not readily available in nature. This concept is widely studied in electromagnetics¹ and the application to acoustic waves raises a growing interest nowadays. Acoustic metamaterials can be designed with the inclusion of elements whose dimensions are smaller than the wavelength in a host waveguide. Then, the processed macroscopic parameters can have negative values and new phenomena can be observed, like negative refraction.

In the domain of electromagnetics, two kinds of metamaterials can be described: arrays of resonant inclusions and transmission line based metamaterials. In the literature, the category of resonant inclusions is the most reported to date.

Our study proposes to develop a structure belonging to the second kind of materials which exhibits desired meta-properties over a much larger bandwidth and with lower losses than the first one.

Thus, a one-dimensional negative refractive index acoustic metamaterial based on the dual transmission line concept has been recently introduced². It is composed of an acoustic waveguide periodically loaded with membranes having the function of series capacitances and transversally connected open channels (referred to as stubs) having the function of shunt inductances. This structure presents negative refraction over almost one octave from 0,6 to 1 kHz, and a “positive behavior” above 1 kHz, without discontinuity between these two domains. This paper presents design and numerical modeling issues associated with this kind of structures.

After explaining the transmission line concept, the membrane and the stub are described and characterized. To that purpose, lumped and finite element models have been realized, where the first ones are based on Kirchhoff formulation (enabling electroacoustic analogies) and the last ones are realized with Comsol Multiphysics®. Then, the design of the acoustic metamaterial is presented and validated owing to the computation of Bloch and scattering parameters.

2 Conventional and dual acoustic TL

Transmission line concept, denoted TL, enables us to describe the propagation of waves in different systems. This chapter presents the convention used for a conventional medium and introduces the concept of a TL-based metamaterial. In the acoustic circuit modeling used in this work, the acoustic pressure corresponds to the voltage and the volume velocity to the current. In the following, we assumed a time dependence in $e^{j\omega t}$.

2.1 Conventional acoustic TL

With this convention, an incremental section dz of a conventional fluid can be represented by an acoustic mass m_a and an acoustic compliance C_a (see Figure 1) where ρ and K are the density and the bulk modulus of the fluid and S , the cross-sectional area.

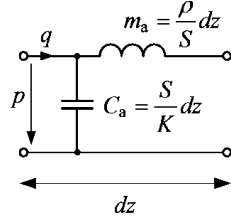


Figure 1 - Incremental circuit for a conventional medium

The characteristic impedance Z_{ac} of this TL is given by

$$Z_{ac} = \frac{Z_c}{S} = \frac{\rho c}{S} \quad (1)$$

where Z_c is the characteristic acoustic impedance of the considered medium and c , the speed of sound.

In this work, the considered medium is air whose parameters are given in Table 1.

Symbol	Value	Unit
ρ	1.188	kg/m ³
c	340	m/s
K	137.4	kPa
Z_c	404	Pa.s/m

Table 1 - Air parameters

2.2 Dual acoustic TL

Figure 2 shows the dual topology of the conventional TL, which is often referred to as the dual TL and which exhibits a negative refractive index over an infinite bandwidth.

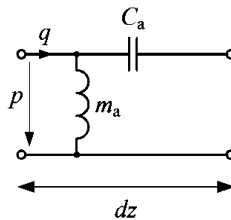


Figure 2 - Incremental circuit for a dual medium

However, the dual TL cannot be realized in this way, it has to load a conventional TL. In other words, the shunt acoustic mass m_{ap} and series acoustic compliance C_{as} (Figure 3) of the

dual TL have to be connected with the elements of the conventional TL: series acoustic mass m_{as} and shunt acoustic compliance C_{ap} .

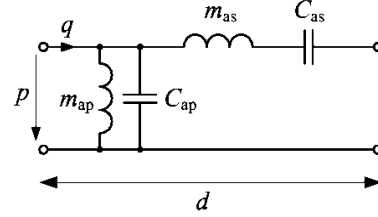


Figure 3 - Unit cell of the composite right/left-handed (CRLH) TL

Because of very small losses in TL-based metamaterials, their equivalent circuits are assumed lossless, that is to say with no small equivalent resistances in these circuits.

The resulting unit-cell has a lattice constant d and is called a composite right/left-handed TL because of the co-existence of the two previous configurations. At low frequency, m_{ap} and C_{as} are predominant, the behavior is left-handed (LH), that is to say with a negative refractive index; whereas in higher frequency, m_{as} and C_{ap} dominate, resulting in a right-handed (RH) behavior with a positive refractive index.

A possible structure implementing the circuit of Figure 3 with acoustic and mechanical elements has been reported in Ref. 2. Moreover, the structure has the particularity of showing a seamless transition (without band gap) between the LH and RH bands, which is called the balanced condition.

3 Description of the proposed structure

The first part of this section describes the realization of series compliance. Using only acoustic elements is not obvious, which is why we propose to use mechanical membranes operating below their first resonance frequency and providing the required series compliances.

In the second part, shunt acoustic mass realized with open channel is presented.

These elements, having the function of dual TL, load a host waveguide of radius $a = 9.06$ mm, representing the conventional TL. The obtained cell has to keep the balanced condition, with a transition frequency $f_0 = 1$ kHz. Moreover, the lattice constant d should be small compared to the wavelength, that is why for having $d/\lambda = 0.1$ at f_0 , we imposed $d = 34$ mm.

According to the equations of Figure 1, the parameters of the host waveguide are

$$\begin{cases} m_a = \frac{\rho}{S} d - h = 156.1 \text{ kg} / \text{m}^4 \\ C_a = \frac{S}{K} d - h = 63.6 \times 10^{-12} \text{ m}^3 / \text{Pa} \end{cases} \quad (2)$$

where h is the thickness of the membrane (see next section).

Finally, one cell of the proposed structure exhibits the equivalent circuit of Figure 3 where the parameters can be expressed with those of the membrane (m_{am} , C_{am}), the stub (m_{at} , C_{at}) and the host waveguide (m_a , C_a):

$$\begin{cases} m_{as} = m_{am} + m_a \\ C_{ap} = C_{at} + C_a \end{cases} \text{ and } \begin{cases} m_{ap} = m_{at} \\ C_{as} = C_{am} \end{cases} \quad (3)$$

3.1 Realization of series compliances with membranes

3.1.1 Lumped element model of the membrane

For the realization of the acoustic series compliance, we propose to build a thin circular membrane clamped at its perimeter in a waveguide, as shown in Figure 4.

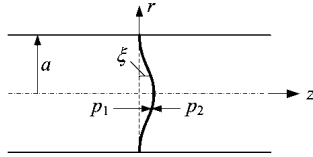


Figure 4 - Cut view of an elastic circular membrane clamped to an acoustic waveguide

The characteristics of this Kapton® membrane are its Young's modulus E_m , Poisson's ratio ν_m and mass density ρ_m . Its dimensions are its radius a (same as the host waveguide) and thickness h , whose values are given in Table 2.

Symbol	Value	Unit
E_m	2.758	GPa
ν_m	0.34	-
ρ_m	1420	kg/m ³
a	9.06	mm
h	125	μm

Table 2 - Parameters of the membrane

These dimensions are chosen in order to have the resonance frequency $f_0 = 1$ kHz for the series branch of the equivalent circuit presented in

Figure 3 with the expressions for the elements detailed in (3), that is to say

$$f_0 = \frac{1}{2\pi\sqrt{(m_{am} + m_a)C_{am}}} = 1000 \text{ Hz} \quad (4)$$

where the expressions of the mass m_{am} and compliance C_{am} are given in (6).

Under the first resonance frequency f_r of the membrane, which is

$$f_r = 0.4694 \frac{h}{a^2} \sqrt{\frac{E_m}{\rho_m(1-\nu_m^2)}} = 1059 \text{ Hz} \quad (5)$$

its impedance Z_{am} can be accurately approximated by a series resonant circuit composed of an acoustic mass m_{am} and compliance C_{am} (see Figure 5).

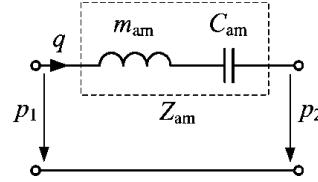


Figure 5 - Equivalent circuit modeling of this membrane

The values of these elements can be expressed against the parameters as²

$$\begin{cases} m_{am} = 1.8830 \frac{\rho_m h}{\pi a^2} = 1296 \text{ kg} / \text{m}^4 \\ C_{am} = 0.0611 \frac{\pi a^6 (1-\nu_m^2)}{E_m h^3} = 17.43 \times 10^{-12} \text{ m}^3 / \text{Pa} \end{cases} \quad (6)$$

3.1.2 Finite element model of the membrane

The membrane loading the host waveguide is modeled in a 2D axi-symmetric acoustic structure interaction model. It is composed of a mechanical model, which processes the displacement of the membrane, and a pressure acoustic one, which computes the reaction of air. These two models interact each other during solve process.

The material, air parameters and dimensions are those given in Table 1 and Table 2, and for ease of modeling, no tension is applied to the membrane which is modeled as a thin plate. The host waveguide lateral boundaries are modeled with perfect rigid walls, with the option "Sound Hard Walls". On one side of it, a source of pressure of $P_0 = 1$ Pa is applied. On the other side, the output is under the condition of plane wave radiation, with the option "Radiation Condition".

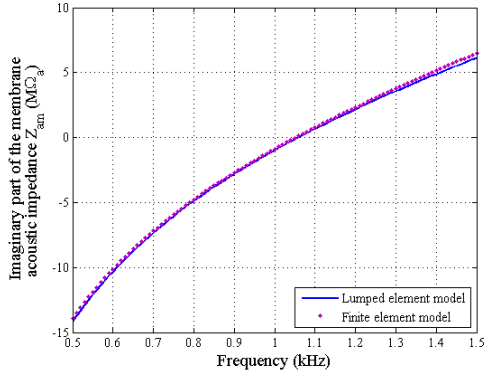


Figure 6 - Imaginary part of Z_{am}

The plane wave propagation in the tube is assured for frequencies satisfying

$$f < 0.586 \frac{c}{2a} = 1 \text{ kHz} \quad (7)$$

Then, the membrane acoustic impedance is obtained in Comsol Multiphysics® by

$$Z_{am} = \frac{\Delta p}{Sv} \quad (8)$$

where Δp is obtained by computing the difference between the average pressure applied on each sides of the membrane, v is the average velocity of the membrane and S its area. The results are compared with lumped element model in Figure 6. Only the imaginary part is presented because equivalent circuits are assumed lossless, as explained in section 2.2.

We can notice a good matching and that under f_r , its behavior is mainly governed by C_{am} , the series compliance. This is one of the two elements necessary for a dual transmission line.

3.2 Realization of shunt masses with stubs

3.2.1 Lumped element model of the stub

Shunt acoustic mass can be realized with short open tube, denoted stub, transversally connected to the main host waveguide. For simplifying the model, we consider a structure that exhibits a perfect symmetry of revolution. As shown in Figure 8, the stub is a short radial waveguide of length L and thickness b connected to the main acoustic circular waveguide of radius a . The values are given in Table 3.

Symbol	Value	Unit
L	48.95	mm
b	1	mm

Table 3 - Parameters of the stub

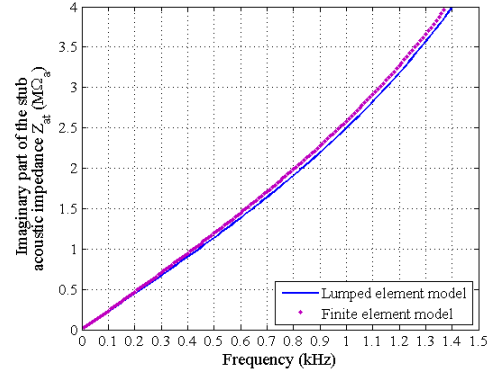


Figure 7 - Imaginary part of Z_{at}

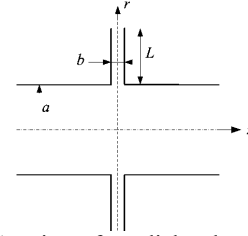


Figure 8 - Cut view of a radial stub connected to an acoustic circular waveguide

These dimensions are chosen in order to have the resonance frequency $f_0 = 1$ kHz for the parallel branch of Figure 3, that is to say

$$f_0 = \frac{1}{2\pi\sqrt{m_{at}(C_{at} + C_a)}} = 1000 \text{ Hz} \quad (9)$$

where m_{at} and C_{at} are the elements of the parallel admittance $Y_{at} = 1/Z_{at}$ loading the host waveguide and used to establish the model of the stub. At low frequency, the admittance can be approximated by an acoustic mass. However, to be more accurate in higher frequency, a compliance can be added (see Figure 9).

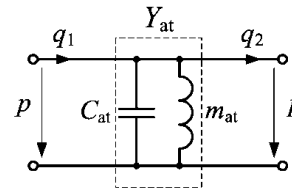


Figure 9 - Equivalent circuit modeling of this stub

To respect the condition $f_0 = 1$ kHz, the value of C_{at} should be set as follows, owing to (9). The expression of m_{at} can be found in Ref. 2.

$$\begin{cases} m_{at} = \frac{\rho}{2\pi b} \ln\left(1 + \frac{L}{a}\right) = 351.1 \text{ kg} / \text{m}^4 \\ C_{at} = \frac{1}{4\pi^2 f_0^2 m_{at}} - C_a = 8.34 \times 10^{-12} \text{ m}^3 / \text{Pa} \end{cases} \quad (10)$$

3.2.2 Finite element model of the stub

The stub loading the host waveguide is modeled in a 2D axi-symmetric acoustic pressure model. The dimensions are b and $L_c = 42.67$ mm because of the termination effects. Indeed, the output of the stub is modeled as an open termination radiating in a surrounding medium that is why the length has to be decreased to obtain the same acoustic mass as in the lumped element model (where this medium is not taken into account). The border of the medium is under the option “Radiation Condition”, like the output of the waveguide whose walls are still perfectly rigid and which is under the same source pressure.

The impedance of the stub is obtained by

$$Z_{at} = \frac{P}{Sv} \quad (11)$$

where p is the average pressure at the entry of the stub and v the average velocity at the same location. The results are compared to lumped element model in Figure 7. A good matching is also obtained. This enables us to use our models to compute the complete TL-based metamaterial.

4 Realization of the CRLH TL

4.1 Lumped element model of the CRLH TL

The realization of the acoustic TL-based metamaterial is made by the combination of the previous structures, as we can see on Figure 10. It has to terminate at both sides by a stub of thickness $b/2$ to be a structure composed by symmetric cells.

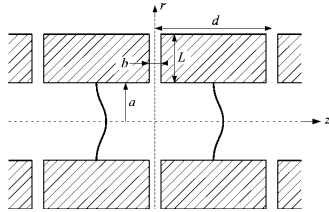


Figure 10 - Cut view of the CRLH TL

By using the lumped element models presented before, one cell of this structure can be expressed with a lumped element model described in Figure 11.

Below f_0 , the proposed structure has to behave as a dual TL, in other words the acoustic series compliances and shunt masses have to be predominant. Above this frequency, the other elements dominate, consisting in a conventional

TL. According to (3), the values of these elements are given in Table 4.

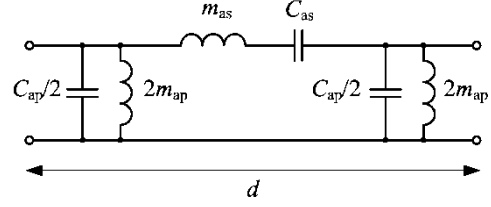


Figure 11 - Lumped element model for the symmetrical Pi-type unit cell of the CRLH TL

Symbol	Value	Unit
m_{as}	1452.1	kg/m ⁴
m_{ap}	351.1	kg/m ⁴
C_{as}	17.43×10^{-12}	m ³ /Pa
C_{ap}	71.94×10^{-12}	m ³ /Pa

Table 4 - Values of masses and compliances

In order to have a balanced condition, we should verify the condition

$$m_{as} C_{as} = m_{ap} C_{ap} \quad (12)$$

The length of the stub L_c is adjusted to 43.5 mm to achieve this condition.

4.2 Finite element model of the CRLH TL

The complete model is also 2D axi-symmetric. It is an acoustic structure interaction model composed of a mechanical one and a pressure acoustic one.

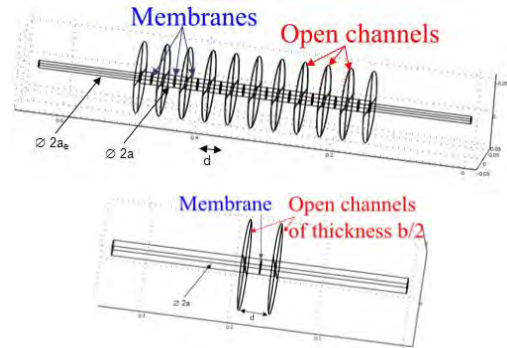


Figure 12 - View of the proposed CRLH TL combining membranes and radial open channels. (up) 10 cells. (bottom) 1 symmetric cell.

The source of pressure is set to $P_0 = 1$ Pa and the propagation is always under plane wave. The output of the host waveguide is modeled with no reflection, whereas the stub radiates in a surrounding medium. The CRLH TL is connected to a waveguide with a radius $a_e = 5.54$ mm to obtain a good adaptation at the interfaces.

5 Methodologies for the acoustic performances assessment

In order to check the behavior of the CRLH TL, the Bloch parameters can be calculated for only one cell. These parameters are the dispersion diagram $\gamma_B d$ and the Bloch impedance Z_B which described the propagation in periodic structures. The calculations are made by lumped and finite element models which are described in this section and the results are presented in the next one.

5.1 Assessment by lumped element model

The pulsations ω_R and ω_L of the two branches can be expressed owing to the series and parallel elements¹:

$$\omega_R = \frac{1}{\sqrt{m_{as} C_{ap}}} \text{ and } \omega_L = \frac{1}{\sqrt{m_{ap} C_{as}}} \quad (13)$$

This enables to write the relations:

$$\chi = \frac{\omega}{\omega_R} - \frac{\omega_L}{\omega} \text{ and } Z_R = \sqrt{\frac{m_{as}}{C_{ap}}} \quad (14)$$

Then, the index of propagation and the impedance are obtained by

$$\begin{cases} \cos(\gamma_B d) = 1 - \frac{\chi^2}{2} \\ Z_{B,\pi} = \frac{Z_R}{\sqrt{1 - \frac{\chi^2}{4}}} \end{cases} \quad (15)$$

5.2 Assessment by finite element model

In the finite element model, four probes are placed for sensing the pressure, as showed in Figure 13.

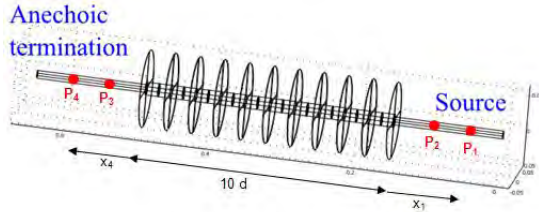


Figure 13 - Finite element model of the CRLH TL

Their positions are given in Table 5 and the distance s between the microphones 1 and 2, 3 and 4 is also useful for the calculation:

$$s = x_1 - x_2 = x_3 - x_4 = 0.05 \text{ m} \quad (16)$$

Symbol	Value	Unit
x_1	0.1	m
x_2	0.05	m
x_3	-0.05	m
x_4	-0.1	m

Table 5 - Positions in the finite element model

The methods of the two and four microphones are used for computing the reflection and transmission coefficients. Please refer to Ref. 4 and Ref. 5 for more details.

For the reflection coefficient R , only the microphones 1 and 2 are used.

For the transmission coefficient T , we consider A , the incident wave component in the upstream tube and C , the transmitted wave component in the downstream tube.

We obtain the following relations for these coefficients:

$$\begin{cases} R = \frac{H_{12} - e^{-jks}}{e^{jks} - H_{12}} e^{2jks_1} \\ T = \frac{C}{A} = \frac{P_3 e^{jks_4} - P_4 e^{jks_3}}{P_1 e^{jks_2} - P_2 e^{jks_1}} \end{cases} \quad (17)$$

where $H_{12} = P_2/P_1$ and P_i is the pressure at the microphone i .

Owing to these coefficients, we can also determine the Bloch parameters using a single cell. Indeed, the scattering matrix S of one symmetric and reciprocal cell can be written

$$S = \begin{bmatrix} R & T \\ T & R \end{bmatrix} \quad (18)$$

Thus, the propagation index and the Bloch impedance can be expressed by

$$\begin{cases} \cos(\gamma_B d) = \frac{1 - R^2 + T^2}{2T} \\ Z_B = \pm Z_0 \sqrt{\frac{(1+R)^2 - T^2}{(1-R)^2 - T^2}} \end{cases} \quad (19)$$

6 Performances of the CRLH TL

6.1 Bloch parameters computed for one cell

Only one cell is considered for computing the Bloch parameters $\gamma_B = \alpha_B + j\beta_B$ and Z_B . The refractive index n can be deduced by $n = \gamma_B/(jk)$. They are obtained as described before and the results are presented in Figure 14 and Figure 15. We can notice that these two models match rather well.

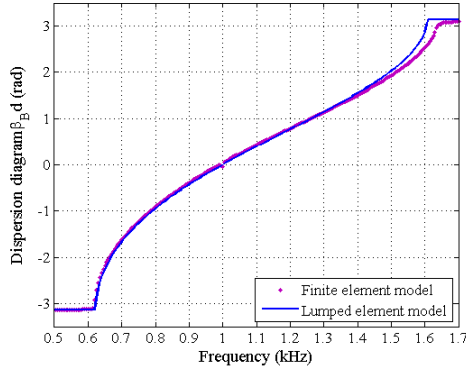


Figure 14 - Dispersion diagram

The structure exhibits a negative refractive index band from 0,6 to 1 kHz followed by a positive refractive index band until 1.6 kHz. Moreover, the balanced condition is obtained, that is to say there is only one frequency for which the refractive index is null.

The Bloch impedance Z_B does not vary much around f_0 . The matching of the metamaterial with the connected waveguide is thus verified, that is to say $Z_{acHWG} = Z_B(f_0) = 4,2 \text{ M}\Omega_a$, and justified the choice of $a_e = 5,54 \text{ mm}$.

6.2 Scattering parameters computed for a 10-cell long structure

A 10-cell long structure has also be modeled and validated owing to finite element model. The reflection and transmission coefficients of this CRLH TL are showed on Figure 16. These results can be used as a reference to estimate the future experimental ones.

7 Conclusion

Circuit theory concepts have been efficiently used to design a TL-based metamaterial. The inclusion of mechanical elements, represented by membranes, seems to be a solution for realizing the series compliances; while the parallel masses have been realized with only acoustic elements.

Thus, the proposed structure exhibits a negative refractive index over almost one octave and a balanced condition between the two different behaviors. These performances have been confirmed by lumped and finite element models in terms of Bloch parameters.

Thereafter, these results have to be validated owing to experimental measurement of reflection and transmission coefficients for a 10-cell long structure with the method of section 5.2.

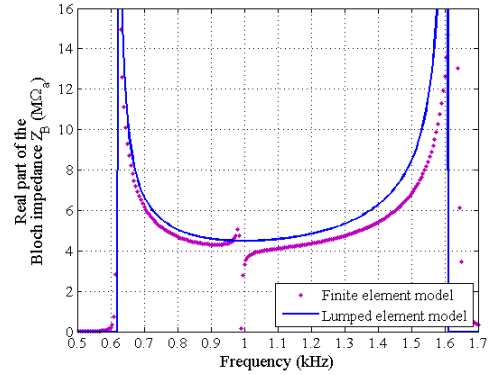


Figure 15 - Real part of Z_B

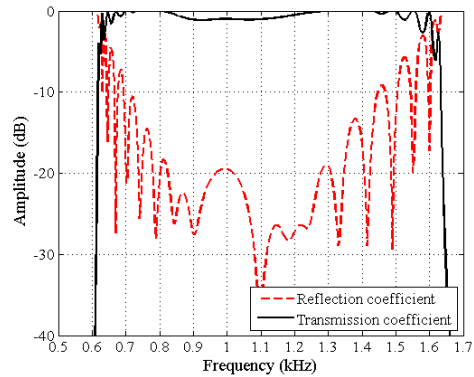


Figure 16 - Reflection and transmission coefficients

Further work will also be done in finite element modeling to predict the performances of a two-dimensional version of this structure.

8 References

1. F. Bongard, Contribution to characterization techniques for practical metamaterials and microwave applications, *Ph.D. Thesis*, Ecole Polytechnique Fédérale de Lausanne (EPFL) (2009)
2. F. Bongard, H. Lissek and J.R. Mosig, Acoustic transmission line metamaterial with negative/zero/positive refractive index, *Physical Review B*, vol. **82**, p. 094306 (2010)
3. M. Rossi, Audio, *Presses polytechniques et universitaires romandes* (2007)
4. A-S. Moreau, H. Lissek and R. Boulandet, Study of an electroacoustic absorber, *COMSOL Conference* (2009)
5. ASTM E2611-09, *Standard Test Method for Measurement of Normal Incidence Sound Transmission of Acoustical Materials Based on the Transfer Matrix Method* (2009)